THE ANNALS OF "DUNAREA DE JOS" UNIVERSITY OF GALATI.
FASCICLE IX. METALLURGY AND MATERIALS SCIENCE
N^0. 1 – 2007, ISSN 1453 – 083X

STUDY OF TRIBOCORROSION PROCESSES BY ELECTROCHEMICAL TECHNIQUES

Lidia BENEA, Viorel DRĂGAN
"Dunărea de Jos" University of Galati
Competences Center Interfaces – Tribocorrosion and Electrochemical Systems (CC-ITES)
email: Lidia.Benea@ugal.ro

ABSTRACT

Tribocorrosion is defined as the chemical-electrochemical-mechanical process leading to a degradation of materials in sliding, rolling or erosion contacts immersed in a corrosive environment. That degradation results from the combined action of corrosion and wear. The mechanism of tribocorrosion is not yet fully understood due to the complexity of the chemical, electrochemical, physical, and mechanical processes involved. Examples of the occurrence of tribocorrosion in service are the accelerated corrosion of steel conveyors exposed to ambient air of high relative humidity, the fall out of electrical connectors in the automotive industry, the degradation of hip prosthesis and dental fillers, the erosion wear of turbine blades, etc. The combined corrosion-wear degradation of materials in sliding contacts immersed in electrically conductive solutions is investigated in-situ by electrochemical techniques. Such techniques are the open circuit potential measurements, E_{OC}, the potentiodynamic polarization measurements, PD and the electrochemical impedance. Capabilities and present limitations of these techniques are discussed based on a tribocorrosion study of a cobalt chromium alloy hard coating (Stellite6) and stainless steel (304L) immersed in water-based electrolytes, namely aerated 0.5 M sulphuric acid, Ringer solution or cooling water reactor (12 ppm Li as LiOH+1000 ppm Boric Acid) and sliding against a corundum counterbody. Some novel insights into the tribocorrosion mechanism of active and passive materials are discussed. These in-situ electrochemical data provide insights into a possible synergism between corrosion and wear processes in sliding contacts. This paper concludes on the benefit of using different electrochemical analyzing techniques when investigating the behaviour of materials under corrosion-wear test conditions.

KEYWORDS: tribocorrosion, active, passive, cobalt-chromium alloy, stainless steel 304L, electrochemical techniques.

1. Introduction

In industry corrosion and wear are responsible for maintenance expenses and loss of productivity resulted from the shortened life of components and catastrophic failure leading to massive costs of the replacement and litigation [1, 2].

Tribocorrosion is defined as the chemical-electrochemical-mechanical process leading to a degradation of materials in sliding, rolling or erosion contacts immersed in a corrosive environment. That degradation results from the combined action of corrosion and wear. The mechanism of tribocorrosion is not yet fully understood due to the complexity of the chemical, electrochemical, physical, and mechanical processes involved. Examples of the occurrence of tribocorrosion in service are the accelerated corrosion of steel conveyors exposed to ambient air of high relative humidity, the fall out of electrical connectors in the automotive industry, the degradation of hip prosthesis and dental fillers, the erosion wear of turbine blades, etc. The evidence of tribocorrosion wear in pressurized water reactors was reported recently by Lemaire and Le Calvar [3]. Some authors have reported on a modification of the surface state of materials in sliding contacts, which results from mechanical, chemical and

electrochemical processes [4-6]. That interaction is of increasing interest since it may result in a new concept of operating materials under lubrication-free sliding or rolling conditions. Indeed, such tribo-reactive surface layers may modify the corrosion process on contacting materials that in turn may modify friction and wear of materials.

Recently, there has been an increase in the interest on the investigation of the combined corrosion-wear degradation of materials by electrochemical methods. The influence of passivity on the tribocorrosion of carbon steel and TiN coatings in aqueous solutions was investigated by Mischler et al. [7, 8]. They used potentiodynamic polarization measurements and performed tests under electrochemical control at different potentials. They concluded that the potential dependence of corrosion-wear is most likely due to the potential dependent lubricating properties of the thin surface films formed in the passivation region. Takadoum [9] investigated the influence of potential on the tribocorrosion of nickel and iron in sulfuric acid solutions. He concluded also that potential affects greatly friction and wear processes. Depending on the applied potential, either corrosion, wear or a conjoint action between them leads to a material loss. Mischler and Ponthiaux [10] reported on a round robin action related to the combined electrochemical and sliding tests on corundum/stainless steel contacts immersed in diluted sulfuric acid. The reproducibility and scattering of their results appeared not to be significantly affected by sliding, and thus they conclude that electrochemical experiments can be correctly carried out in sliding corrosion-wear tests. Watson et al. [11] reported on methods for measuring the corrosion-wear synergism. They proposed penetration rate equations to quantify the wear and corrosion processes as well as the corrosion-wear synergism based on experimentally determined polarization resistance and Tafel slopes. A microelectrochemical technique, in which the current of a metal probe in an electrolyte under rubbing conditions is measured, was proposed by Assi and Böhni [12] to study the corrosion-wear synergy. Their technique allows the study of the repassivation kinetics of surface areas activated by tribocorrosion processes. Ponthiaux et al. [13] used electrochemical noise measurements for the determination of the depassivated area in sliding contacts. They found an interesting correlation between the electrochemical noise and the mechanical processes occurring in sliding contacts. From these investigations it can be concluded that some electrochemical techniques do provide interesting information on the surface state of materials in sliding contacts, but the unravelling of these experimental data towards modelling of tribo-corrosion processes, is still very limited.

That modeling of tribocorrosion is indeed rather limited in literature, and the modeling done does not yet allow a correlation between electrochemical data and material losses in corrosion-wear sliding contacts or a predictive approach of the corrosion-wear synergism. Jemmely et al. [14] proposed an electrochemical modeling of the passivation phenomena in tribocorrosion. That model was developed taking into account the film growth kinetics and the ohmic drop in the electrolyte between wear scar and reference electrode. The model could simulate the general trends observed in current transients but the agreement with experimental data was only fair. Reasons put forward by them are an insufficient insight in the electrochemical conditions in the contact zone and the role of the third body particles. Garcia et al. [15] analysed the corrosion-wear of passive materials in sliding contacts based on a concept of active wear track area in combination with Quinn's mild-oxidation model. Polarization curves were determined under mechanically unloaded and loaded conditions. From that active wear track area and by using repassivation kinetics of bare metals, the material loss in corrosion-wear sliding tests was analysed. Mischler et al. [16] proposed a model that describes the effect of mechanical and materials parameters on the wear-assisted corrosion rate of passive metals under sliding wear conditions. They concluded that to understand the mutual interaction between mechanical and electrochemical parameters affecting wear-accelerated corrosion it is necessary to look at the tribocorrosion system as a whole.

In this paper, an overview of electrochemical and surface analysis techniques of interest for studying specifically the in-situ tribocorrosion process is presented. Experimental data obtained by these electrochemical analysis techniques on the tribocorrosion behaviour of a cobalt chromium alloy hard coating (Stellite6) and stainless steel (304L) immersed in water-based electrolytes, namely aerated 0.5 M sulfuric acid, Ringer solution or cooling water reactor (12 ppm Li as LiOH+1000 ppm Boric Acid) are reported. These two materials are representative for respectively passive and active materials at open circuit potential [17, 18]. The aim is to demonstrate capabilities and present limitations of these techniques for studying the degradation processes of materials in sliding contacts immersed in an electrolyte. Although, attempts are not yet been made to correlate these electrochemical data with material losses in sliding contacts, the in-situ information gathered in this way on the surface state of materials in sliding contacts is expected to support further modelling work.

In many tribocorrosion systems the passivable materials are used. The passive properties of Stellite6

are of great importance in PWR environments, because the nature of the oxide films governs the corrosion release rate and the oxides are involved in plant dosimetry. Chromium enhances passivation of the cobalt alloys and stainless steel, in the presence of oxygen, and is the key ingredient with regard to corrosion resistance in oxidising media.

2. Experimental

Both uni-directional pin-on-disk and ball-on-disk contact geometry have been used in this investigation. Schematic diagrams of the setups are given in Fig. 1. Pin-on-disk and ball-on-disk materials were immersed in the electrolyte and placed in an electrochemical cell containing a counter electrode and a reference electrode. The disks were made of either cobalt chromium alloy (Stellite6) and stainless steel (304L). Stainless steel and cobalt chromium alloy were was selected for their good corrosion resistance that results from the formation of a nanometer thick protective oxide layer (passive film) at its surface in contact with air and or with many oxidizing electrolytes in open circuit potential conditions.

Just before immersion in the electrolyte, the disks were degreased by dipping in alcohol. The pins made of corundum (Al_2O_3), an electrically non-conductive material, were degreased in alcohol and loaded on the disk. All sliding tests were carried out at a constant rotation speed between 30 and 120 rpm. Depending on the tribometer used, friction was generated by applying a load on the rotating disk facing downwards, against the fixed corundum ball (Fig. 1 a), or by rotating the corundum pin against the fixed disk facing upwards (Fig. 1 b).

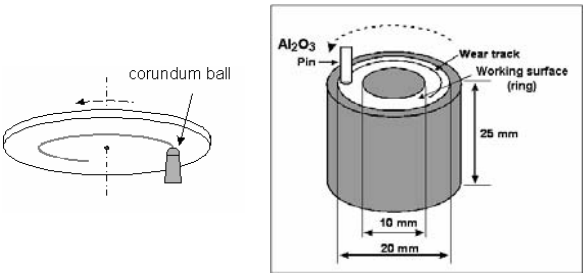

(a) (b)

Fig. 1. *Schematic description of the ball-on-disk (a) and pin-on-disk (b) se-tups used to study Stellite6 and stainless steel respectively*

Despite these differences, the results of the tribocorrosion tests carried out on both tribometers were found to be in very good agreement for the same tribocorrosion conditions (sliding speed or contact frequency, normal load, electrochemical conditions). Such uni-directional sliding conditions lead, in contrast to alternating (bi-directional) contact conditions like fretting [18], to a steady electrochemical condition all over the wear track area on the disk material [4, 17]. That steady state is however quite complex since between the successive passes of the pin or ball, each point on the wear track reacts with the surrounding liquid. Notwithstanding that time-related evolution of the material in the wear track, the achievement of a steady state is revealed by the fact that, if a constant potential value is applied to the metal under friction in the potential range where passivation or dissolution occurs, a steady-state current is obtained. Such a condition is required for the implementation of electrochemical techniques (polarization curves, impedance measurements, etc.).

Corundum as a counter body material in electrochemical tests has a number of advantages. A negligible mechanical deformation of this material takes place on loading onto stainless steel or cobalt – chromium alloy. A negligible wear of the pins or balls occurs, and neither general corrosion of corundum nor galvanic coupling with the counterbody material (in this case the disk material) can take place.

3. Open circuit potential measurements

This method gives information on the electrochemical state of a material, for example active or passive state in the case of stainless steels. However, open circuit potential measurements provide limited information on the kinetics of surface reactions. The open circuit potential recorded during uni-directional pin-on-disk sliding tests, in which the disk is the material under investigation, is a mixed potential reflecting the combined state of the unworn disk material and the material in the wear track. One must be aware that a galvanic coupling between worn and unworn parts on the disk surface may take place [19]. Consequently, the open circuit potential depends on the following parameters:

*The respective intrinsic open circuit potentials of the materials in worn and unworn areas. These open circuit potentials are different because the electrochemical state of the metal is disturbed by the removal of the surface films that may consist of adsorbed species, passive films, or corrosion products, in the sliding contact, and by a mechanical straining of the metal.

*The ratio of worn to unworn areas. In particular, if the extent of the worn area increases, the open circuit potential of the disk will shift depending on the controlling electrochemical processes, being either the anodic (e.g., the dissolution of the metal) or the cathodic reaction (e.g., the reduction of hydrogen or dissolved oxygen).

*The relative position of worn and unworn areas. As a result of the galvanic coupling, a current is flowing between anodic and cathodic areas. The ohmic drop may induce a non-uniform distribution of potential and current density over the disk surface. The measured open circuit potential is thus an average value depending on that distribution.

*The mechanism and kinetics of the anodic and cathodic reactions in worn and unworn areas.

The evolution of the open circuit potential is shown in Fig. 2 for Stellite6 in 0.5 M H_2SO_4 solution at intermittent friction (200 s latency time) with 15N normal force load (F_N) and 120 rpm. The evolution of the open circuit potential was measured under unloaded and mechanically loaded conditions.

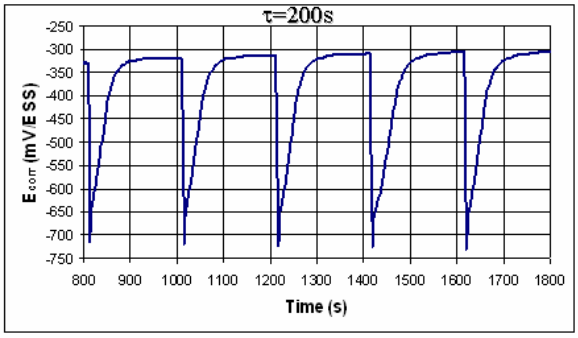

Fig. 2. *Electrochemical measurements of open circuit potential (Ecorr) recorded, during, an unidirectional friction test on Stellite6 with a corundum counterbody in 0.5 M H_2SO_4 solution at intermittent friction (200 s latency time) with 15N normal force load (F_N) and 120 rpm.*

A normal load of 120MPa was applied for 2 s, followed by a latency time (rotation stopped) of 200 s, and this cycle was repeated 2500 times. On immersion, the Stellite6 disk stabilizes at an open circuit potential of −0.32V versus SSE. At the start of the first loading step, a large drop of the potential down to−0.76V versus SSE is noticed. On unloading, the potential increases steeply at first and then at a lower rate, reaching a value of about −0.48V versus SSE after 200 s. This case corresponds to Fig. 2 and an anodic dissolution of the Stellite6 material in the wear track can be expected. The potential of −0.76V versus SSE is re-established during the successive loading steps. Before starting the corrosion-wear sliding tests, the freshly ground and thus active cobalt chromium alloy stainless disk material was immersed for 10^4 sec. In that time interval, a large increase of the open circuit potential of the alloy is noticed. That increase indicates that a stable passive surface state is achieved. At the time the corundum ball is loaded on the rotating alloy disk, a sudden decrease of the open circuit potential takes place (see cathodic shift during friction). The open circuit potential during the corrosion-wear test is quite close to the open circuit potential of the active base material noticed on immersion of the sample in the electrolyte. Finally on unloading of the ball from the disk, the open circuit potential of the stainless steel disk starts to increase (anodic shift) and reaches after some time the initial open circuit potential back. This indicates the re-establishment of a passive state on the surface of the stainless steel material in the wear track area. It should be noticed that the rate at which the open circuit potential decreases on loading and increases on unloading is totally different. The underlying processes are thus different in both cases and have different kinetics. Indeed on loading, a sudden mechanical destruction of the passive surface film is taking place, while on unloading repassivation takes place at a rather limited oxidation rate. It is also interesting to note that the time for initial passivation of the freshly ground surface at the beginning of the test is much longer than the time for repassivation after unloading. At the beginning of the test, the whole surface is in an active state, and a long time is required for passivation in the open circuit potential conditions. On the contrary, after unloading, only a small part of the disk surface in the wear track is active, and a galvanic coupling takes place between this small active area and the rest of the disk surface in a passive state. This coupling induces an anodic polarization of the active area, resulting in an increase of the passivation rate, and a smaller passivation time constant. The typical potential-current response recorded before, during, and after fretting tests performed on AISI 304L stainless steel sliding against corundum in a Ringer solution is shown in Fig. 3.

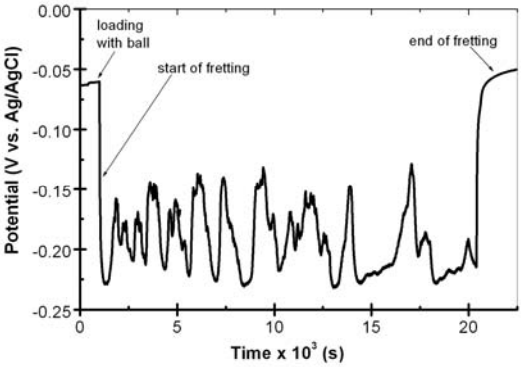

Fig. 3. *Electrochemical measurements recorded before, during, and after a fretting test on AISI 304L stainless steel sliding against corundum in Ringer solution at 1 N, 1 Hz, displacement amplitude of 200 μm, and for 20 000 cycles.*

Under unloaded conditions, the potential variations are quite small and stable. When the ball is loaded on top of the sample, a small decrease in

potential was noticed. At the start of the fretting-corrosion test, the potential of the stainless steel sample undergoes a significant negative shift of about 16 mV. After a running-in phase, the potential fluctuates as long as the fretting-corrosion test was going on. When fretting was ended and the corundum ball was lifted away from the worn surface, the potential of the working electrode returned progressively to the value recorded before the start of the fretting test. Accordingly, the potential and current variations in Figure 3 suggest that the tested stainless steel sliding against corundum under the considered test conditions; mainly undergo a removal of their passive surface film at the start of fretting. They remain partly active during the sliding test, and finally progressively repassivate on unloading. In the case of passivating materials like stainless steel, the potential drop on loading/sliding can be a few hundred millivolts large as it is illustrated in Fig. 3. From Fig. 2 and 3 it can be seen that the open circuit potential of Stellite6 and stainless steel immersed in aqueous solutions decreases on loading and subsequently at the start of a bi-directional sliding test (fretting). That potential drop should not be solely related to a change in free energy, but one should also consider the possible effect of a mechanical degradation of the surface oxide on loading and under sliding. In any case, since loaded and unloaded materials are physically and electrically connected, a mixed potential, E_{mix} is induced. At that mixed potential, anodic and cathodic currents are equal but of opposite sign. Considering that the only possible anodic and cathodic reactions are represented by Eq. (1), an electrochemically induced material transfer takes place between loaded and unloaded areas, consisting of an anodic dissolution and a subsequent cathodic re-deposition.

$$M^{n+} + ne^{-} \Leftrightarrow M \qquad (1)$$

The result is that a net weight loss will thus not be measured although a height difference between loaded and unloaded areas will appear.

From this analysis of the electrochemical behaviour of materials in partially mechanically loaded conditions, some reflections on synergism in tribocorrosion can be formulated. The definition of synergism in corrosion-wear, W_{synerg} as proposed by Stack and Pungwiwat [xx 9] is:

$$W = W_{mechan} + W_{corr} + W_{synerg} \qquad (2)$$

Where W is the weight loss in tribocorrosion tests, W_{mechan} the weight loss in absence of corrosion and W_{corr} is the weight loss in the absence of wear.

The open circuit potential of passive materials in sliding contacts is quite sensitive to the loading conditions and type of test aqueous solution. The open circuit potential of AISI 304L stainless steel disks immersed in Ringer solution varies largely with normal force and contact frequency (Fig. 4). In unloaded conditions and without any rotation of the disk, the open circuit potential after an initial delay of 6 000s, corresponds to that of disk material in passive state. Once a mechanical contact is established and the disk is rotating, friction occurs and a shift of the open circuit potential towards lower potentials (cathodic shift) is observed. The amplitude of that shift increases with increasing normal force and/or increasing sliding speed or contact frequency.

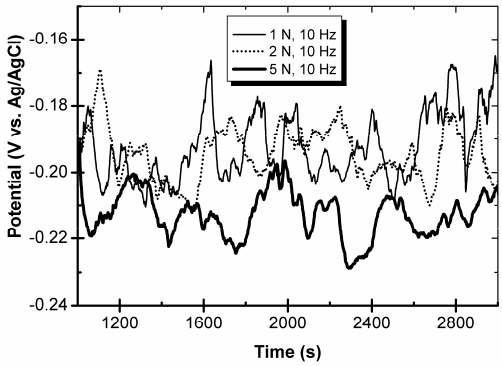

Fig. 4. *Potential variation recorded on AISI 304L stainless steel during fretting-corrosion against corundum in a Ringer solution at 10 Hz, 200 µm, 20000 fretting cycles under different applied normal forces.*

The open circuit potential of cobalt chromium alloy (Stellite6) immersed in 0.5M sulphuric acid is shifted down during fretting with a contact pressure of 120 MPa and 200 s latency time with about 350 mV at room temperature (Fig. 2). For cobalt chromium alloy, immersed in cooling water reactor at 85 ^{0}C and the same fretting conditions, the open circuit potential is shuting douwn during fretting with only 200 mV, see Fig. 5 [20].

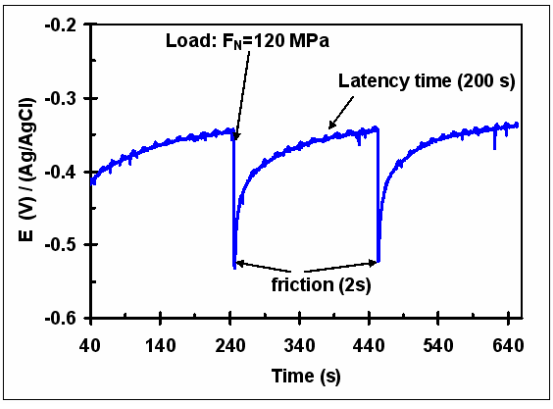

Fig. 5. *Electrochemical measurements of open circuit potential (E) recorded, during, an unidirectional intermittent friction test on Stellite6 with a corundum counterbody in water cooling reactor solution at 85 ^{0}C (200 s latency time) with 15N (120 MPa) normal loading force*

Such a shift in the open circuit potential can be explained as follows:

*The passive film can be partly destroyed (cracking, partial removal) in the contact area under sliding conditions where friction occurs. This may initiate a galvanic coupling between the passive surface layer and the bare base material, with a local dissolution of the base material as a consequence. Since the open circuit potential of active material is cathodic compared to passive material, the open circuit potential of partially depassivated materials shifts towards the active region.

*The contact area (Hertzian contact area) between the first bodies increases at increasing normal load. The increase of the normal load generates a larger wear track area and a larger active area. The lowering of the open circuit potential can be explained by the increase of the active-to-passive area ratio.

*The variation of the open circuit potential with contact frequency is linked to the time interval between two successive contact events during which material in the wear track may repassivate. At higher contact frequency, the amount of active material in the wear track area thus increases. This results in a cathodic shift of the open circuit potential due to an increased ratio of active-to-passive area.

Variations of the open circuit potential of materials subjected to sliding conditions can thus be correlated with variations in the surface conditions of the material under investigation. However, a detailed interpretation of open circuit potential measurements is difficult. Indeed, the open circuit potential is an average value determined by factors as the ratio active-to-passive material in the wear track, the repassivation kinetics of the base material, the contact frequency, and the normal load. As a consequence, the local surface conditions of the material in and outside the wear track cannot be precisely derived from open circuit measurements unless more detailed electrochemical data on passive and active material become available. Such information on the local tribological and electrochemical conditions across a partly worn surface could be gained from a precise knowledge on the potential distribution over that surface.

Microelectrodes could be helpful in that respect. Some reviews are available showing the use of such microelectrodes to investigate localized corrosion [12] and corrosion-wear [18]. However, the interpretation of the variation of open circuit potential and potential distribution requires kinetic data to characterize the electrochemical reactions occurring on active and passive materials. Such kinetic data can be acquired by electrochemical techniques such as potentiodynamic polarization and electrochemical impedance measurements.

4. Potentiodynamic polarisation measurements

Potentiodynamic polarization measurements can be used to derive the dependence of anodic or cathodic current, I, on the electrode potential, V, measured *vs*. a reference electrode. This method is useful in determining the active/passive behaviour of materials at different potentials.

Such potentiodynamic polarization curves obtained at increasing potential dV/dt (direct scan) on cobalt chromium alloy (Stellite6) immersed in 0.5 M sulfuric acid is shown in Fig. 6. Two cases are shown, namely one (1) without any external loading and one (2) in contact with a sliding corundum ball loaded at 15 N. Both curves were recorded after the open circuit potential of the alloy has reached the passive value [17, 20].

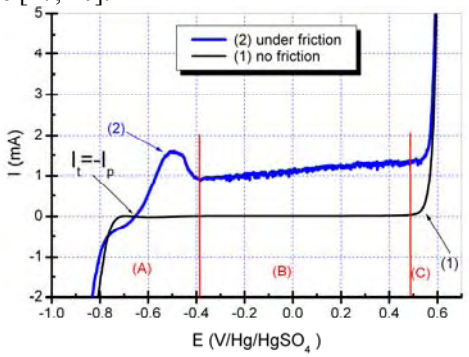

***Fig. 6**. Potentiodynamic polarization curves of Stellite6 in H2SO4 0.5M recorded by direct potential scan, from −1.0 to +0.6 V/SSE, at 0.1 V/min. Curve (1): no friction applied. Curve (2): continuous friction (10 N; 120 rpm).*

If the stellite surface of the specimen is not subjected to rubbing (curve 1), hydrogen evolution and oxygen reduction are the only reactions detected in the potential domain A. In domain B, the alloy was passivated, and the current remained very small (<10μA). The zero-current potential lay between −0.3 and −0.5 V/SSE. In domain C (potential >0.4V/SSE), the anodic current increases with the applied potential, revealing the dissolution of the alloy, induced by oxidation of the Cr^{3+} cations of the passive film, giving soluble Cr^{6+}. When friction is applied (curve 2), the shape of the polarization curve changes: hydrogen evolution on Stellite6 is not modified in domain A, but an anodic current of about 0.5–1.0mA appears in the potential range from [−0.75; +0.5] V/SSE, indicating dissolution of the alloy. A first approach for interpreting the polarisation curve under friction can be developed from the following considerations, based on a concept of "**active wear track**" [15]:

-The measured current, I can be considered as the sumof two partial currents I_t and I_p:

$$(I = I_t + I_p) \quad (3)$$

Where: I_t is the current originated from the wear track areas where the passive film is destroyed and metal is active, and I_p the current linked to the surface not subjected to friction and that remains in passive state.

-At the zero-current potential (−0.75 V/SSE) where I = 0, a galvanic coupling is established. I_t and I_p are different from zero, and $I_p = -I_t$. These partial currents flow between the active wear track areas and the rest of the surface. On the wear track, where dissolution of the material and the formation of a new passive film occur, I_t is anodic. On the remaining surface, I_p is cathodic and is related to reactions such as dissolved oxygen or hydrogen reduction.

-When the potential increases, the galvanic coupling is broken and I_t is no longer equal to $-I_p$. Both I_t and I_p increase. As a result, the measured current I, flowing between the specimen and the counter electrode increases.

On the surface not subjected to friction and in passive state, I_p cannot exceed the value of the current measured at the same potential on the unrubbed specimen. By comparing the values of I in both conditions (see Fig. 6), it can be deduced that, under friction, $I = I_t$ (from −0.7 to 0.5 V/SSE). The total current measured under friction and its evolution with applied potential, are characteristic of the behaviour of material in the wear track. The steep increase of the current with potential around the zero-current potential indicates that a rapid dissolution occurs in the wear track.

The further decrease of the dissolution current above −0.6 V/SSE reveals the effect of repassivation in the active wear track.

The rate of this reaction, occurring in the areas where the passive film is removed, increases with potential. This induces a lowering of the total depassivated area, and thus a decrease of the dissolution current.

The same potentiodynmic curves recorded for Stellite6 in cooling water reactor (12 ppm Li as LiOH+1000 ppm Boric Acid) at 85^{0}C reveals a different behaviour see Fig. 7.

For the curve (1) recorded without fretting we can see the passivation domain. When friction is applied (curve 2 at 30 MPa) and curve (3 at 120 Mpa), the shape of the polarization curve changes. In the passive domain we observe that a continuous dissolution of alloy occurs instead of a passivation, even if we have the same parameters of sliding (Contact pressure and rotation speed of counter body).

Thus, polarization curves reveal the occurrence of depassivation and dissolution of the alloy induced by friction in the wear track, and give the opportunity of quantitative measurements concerning the variation of the active wear track area with tribological parameters (normal load, sliding speed, etc.) [20, 21].

Both effects can be explained by an increase of the area depassivated by friction. At increasing sliding speed, the area depassivated per unit of time increases whereas the restoration rate of the passive film remains constant. On the other hand, at increasing normal loads the contact area where destruction of the passive film occurs, increases, and as a result the total active area also increases.

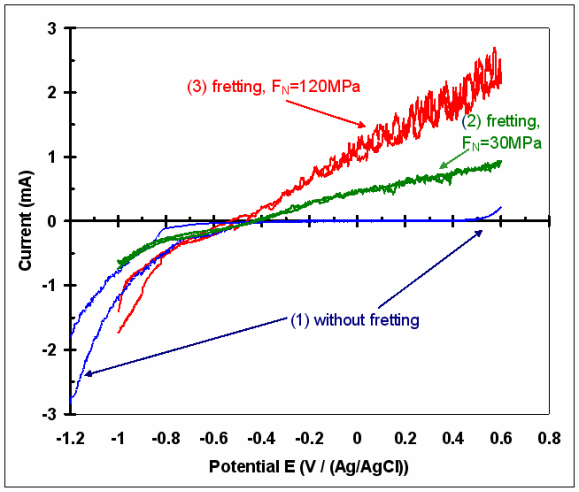

***Fig. 7**. Potentiodynamic polarization curves of Stellite6 in cooling water reactor, recorded by direct potential scan, from −1.0 to +0.6 V/SSE, at 0.1 V/min. Curve (1): no friction applied. Curve (2): continuous friction at 30 Mpa; Curve (3) Continuous friction at 120 Mpa Rotation speed 120 rpm*

Potentiodynamic current potential curves recorded on Stellite6 allow the prediction of the huge influence of friction on the total wear rate in tribocorrosion conditions. One possible synergy between the processes governing wear and corrosion can be pointed out, namely the local destruction of the passive film in the contact area that increases the corrosion rate of the material by several orders of magnitude. Consequently, when a metal is "active" in a corrosive medium, the influence of friction on its electrochemical behaviour can not be neglected. Synergy between friction and corrosion must be considered.

Polarization curves are thus useful in tribocorrosion studies in so far as they give information on changes in electrochemical reaction kinetics induced by sliding, and also on the influence of the surface reactions on the sliding conditions in the contact. The interpretation of polarization curves

has similar limitations as those encountered in the interpretation of open circuit potential measurements, namely due to the coexistence of galvanic coupling of worn and unworn areas. However, by considering carefully the heterogeneous state of tribological surfaces, polarization curves in tribocorrosion studies can yield detailed quantitative information on aspects as mechanical depassivation of worn surfaces, local and overall corrosive wear rates, and the mechanism of mechanical wear under various tribological conditions [17, 18].

Nevertheless, tribocorrosion in field conditions essentially occurs at open circuit potential. However, in most laboratories electrochemical tests are performed under polarization and not at open circuit potential. One possible solution is to use electrochemical impedance spectroscopy (E.I.S.). That method allows a thorough investigation of the corrosion mechanism and the kinetics under open circuit conditions. The measurement of the electrochemical impedance is made by using a sinusoidal voltage signal with small amplitude (5 to 10 mV). This has the advantage of generating only a negligible perturbation on the open circuit potential of the material tested.

5. Electrochemical Impedance Measurements

It is interesting to compare the impedance diagrams corresponding to a totally active surface (diagram 1) and to a totally passive surface (diagram 2). The size of the impedance diagrams differs by several orders of magnitude, particularly in the "low frequency range" (typically < 0.1 Hz). A classical interpretation of impedance diagrams consists in relating the corrosion current, I_c, on a given area, A, to the charge transfer resistance, R_{ct} [22, 23], which is a parameter of the electrochemical impedance that can be deduced from the experimental diagrams:

$$I_c = \frac{B}{R_{ct}} \qquad (4)$$

B is a constant factor related to the corrosion or passivation mechanism (value between 25 and 50 mV) [23]. In the case of diagrams consisting of a single arc of circle, the charge transfer resistance R_{ct} is also the polarization resistance, R_p (R_{ct} = R_p), defined as the limit of the impedance Z_i of metal-electrolyte system when the frequency tends to zero:

$$R_{pol} = \lim_{\omega \to 0} Z_i \qquad (5)$$

In the case of diagrams as in Fig. 8, the polarization resistance is directly related to the size of the semi-circle. The polarization resistance corresponds to the value of the impedance at very low frequencies.

Impedance diagram from Fig 8, recorded before passivation of the Stellite6 alloy at active potential value E=-700 mV vs. Ag/AgCl, corresponds to a totally active surface. The electrical equivalent circuit describing the surface in active state is presented in Fig. 9. By simulating the experimental data with this equivalent circuit we calculated the charge transfer resistance corresponding to active state of the alloy surface, R_{ct}=4.48 kΩcm^2. R_e=1.48kΩ is the electrolyte resistance, and CPE is the capacitive element depending on frequency.

According to equation (4), the corrosion current I_c is 1.42x10^{-9}A (with B=25 mV). Considering the total area of the specimen (4.9cm^2), the corrosion current density i_c is 0.28x10^{-9}Acm^{-2}.

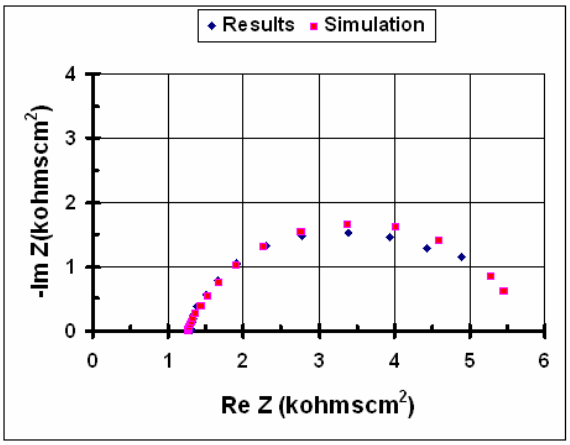

Fig 8. *Nyquist representation of impedance measurements of Stellite6 alloy in water cooling reactor at 85 ^{0}C, recorded at active potential value E=-700mV vs Ag/AgCl, in active state of the surface: (▲) experimental data; (■) fitting diagram*

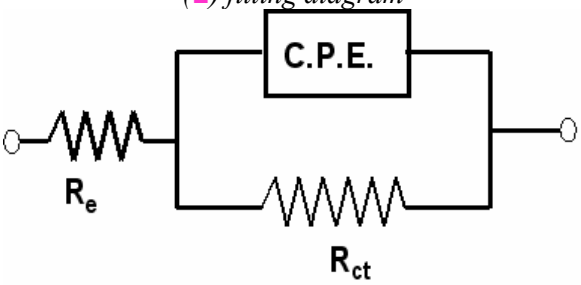

Fig. 9. *Equivalent electrical circuit representing the impedance of the Stellite6 alloy in the active state, immersed in cooling water reactor at 850C, at potential value E=-700 (mV/Ag/AgCl)*

Impedance diagram from Fig. 10 have been recorded after passivation and before applying the friction, corresponds to a totally passivated surface of Stellite6 alloy in cooling water reactor at 85^{0}C, recorded at passive potential E=0.00V(Ag/AgCl).

The electrical equivalent circuit describing the alloy surface in the passive state is similar with those presented in Fig. 9. Instead of a charge transfer resistance, R_{ct}, we have now the polarisation resistance, R_p. By simulating the experimental data with this equivalent circuit we calculated the polarisation resistance corresponding to passive state of the alloy surface, R_p=264.9 kΩcm^2. R_e=1.3 kΩ is the electrolyte resistance, and CPE is the capacitive element depending on frequency.

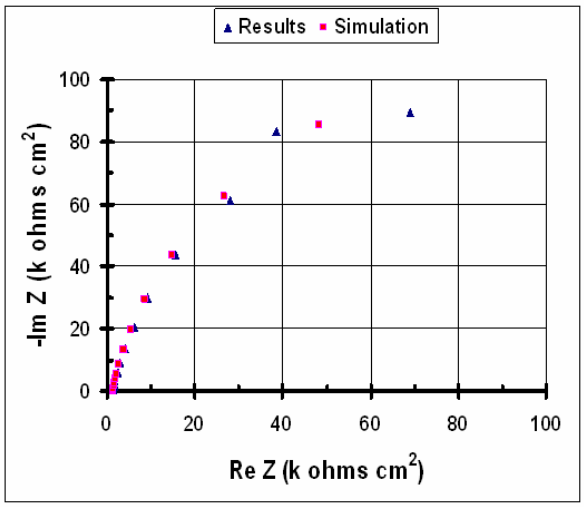

Fig 10. *Nyquist representation of impedance measurements of Stellite6 alloy in water cooling reactor at 85 ^{0}C, recorded atpassive potential value E=-700mV vs Ag/AgCl, in passive state of the surface: (▲) experimental data; (■) fitting diagram*

The residual corrosion current (passivation current) can be assessed by equation (4) from the value of R_p determined on the diagram from Fig 10 after simulation and fitting (R_p = 264.9x10 ohms) so that I_c=8.42x10^{-10}A (with B=25mV) corresponding to a corrosion current density i_c=1.71x10^{-10}Acm^{-2}.

In the case of friction tests we have on the surface both areas: active area corresponding to the wear track and the remaining passive area. This aspect can be interpreted by a simple model based on an equivalent electrical circuit of the impedance of the sample undergoing the tribocorrosion test (Fig. 11).

In a first approach, the global impedance of the sample is considered as a parallel connection of impedances Z_a (corresponding to the active surface) and Z_p (corresponding to the passive surface). Z_a represents the impedance of the material in an active electrochemical state (where the passive film was destroyed by friction, for example), and Z_p the impedance of the surface still covered by a passive film.

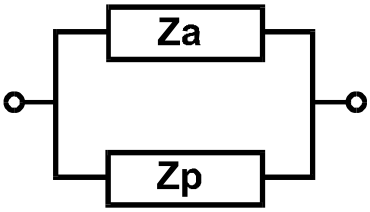

Fig. 11: *Equivalent electrical circuit representing the impedance of the sample surface by a parallel combination of the impedance of the active and passive areas (Z_a and Z_p respectively).*

For such a model, the global impedance is given by:

$$\frac{1}{Z} = \frac{1}{Z_a} + \frac{1}{Z_p} \qquad (6)$$

It must be noticed that this relation is valid over the whole frequency range, and in particular at very low frequencies where $Z \cong Z_i = R_p$. Consequently, a relation similar to equation (5) can be derived for the polarization resistance R_{pol}, $R_{pol/active}$, and $R_{pol/passive}$ being the polarization resistances relative to the total area, the active area and the passive area respectively.

If one assumes that the electrochemical activity of the area depassivated by friction is the same as the one of the active surface before friction, the value of the current density i_c can be used to evaluate the active area A_a. The impedance measurements carried out during tribocorrosion tests illustrate the usefulness of this method to study the mechanism of electrochemical reactions involved in tribocorrosion processes, and the interaction between corrosion and friction. More detailed information on tribocorrosion processes are expected from a systematic study of impedance diagrams recorded at varying tribological test conditions (variation of the normal force, sliding speed, rotation frequency, etc.). The interpretation of impedance measurements recorded during sliding tests is difficult due to the heterogeneous state of the surface, as in the case of polarization measurements. In fact, a non-uniform distribution of the electrochemical impedance over the disk surface must be considered. The action of friction can be thoroughly analyzed, only if this distribution is known. In tribocorrosion experiments, a local analysis of the electrochemical state is thus necessary to interpret impedance measurements. Research work on electrochemical systems with a non uniform distribution of the electrochemical impedance is available now [24]. Such measurements and models can be adapted to tribocorrosion conditions. In that field, microelectrodes could help to map the electrochemical impedance on disk surfaces. Electrical equivalent circuit models or finite element

models could be used to get distributions of impedance, and to calculate the overall impedance.

6. Conclusions

This overview points out the capabilities of electrochemical methods like open circuit potential measurements, polarization curves, and EIS measurements, for the *in situ* investigation of materials used under tribocorrosive conditions in sliding contacts.

They can provide not only essential information on the surface conditions of materials in sliding contacts, but also on the kinetics of reactions that control the corrosion component in the material loss during tribocorrosion tests.

Aspects of the tribocorrosion mechanism that can be clarified in this way are the nature of electrochemical reactions, the formation of protective passive surface films, the interactions between electrochemical reactions and friction. Information can also be gained on kinetics such as corrosion rate, rate of depassivation by mechanical action in the contact area, and rate of repassivation.

Electrochemical methods in tribocorrosion are still facing a few limitations related to the particular conditions of tribocorrosion tests, mainly the heterogeneous state of the surface subjected to sliding, and the time evolution of the wear track area.

In most tribocorrosion tests, in particular sliding tests, only a fraction of the disk is undergoing sliding. The risk of a galvanic cell (corrosion cell) between the wear track area and the rest of the disk surface must be considered. That galvanic cell may induce an electrochemical potential distribution over the disk affecting the rate of electrochemical reactions in the wear track and on the rest of the disk.
This can even destabilize a protective passive film. In such an extreme case, friction applied on a limited fraction of the surface of a passive material may induce a general corrosion over the entire surface.

The time evolution of the wear track material is determined by the contact conditions (unidirectional, bi-directional, intermittent, continuous, etc.).

Notwithstanding the fact that steady state conditions can be obtained during a limited time, it must be considered that at the local scale on every point of the wear track, transient electrochemical conditions are encountered. Measurement procedures, data analysis and modeling must take into account such local transient and periodic aspects. A full understanding of the tribocorrosion mechanisms requires thus a in-depth analysis of and correlation between electrochemical data, surface analyses, and material degradation.

References

[1] A. V. Levy, Surf.Coat. Technol. 36 (1988) 387.
[2] A. J.Ninkam, A. V. Levy, Wear 121 (1988) 347.
[3] E. Lemaire and **M. Le Calvar**, Wear, 249 (2001) 338.
[4] B. **W. Madsen**, Wear, 171 (1993) 271.
[5] X. X. Jiang, S. Z. Li, D. D. Tao, J. X. Yang, Corrosion, 49 n 10 (1993) 836.
[6] T. C. Zhang, X. X. Jiang, S. Z. Li, X. C. Lu, Corrosion Science 36 n°12 (1994) 1953.
[7] S. Mischler, A. Spiegel, M. Stemp and D. Landolt, Wear, 251 (2001) 1295.
[8] S. Barril, S. Mischler and D. Landolt, Tribology International, 34 (2001) 599.
[9] J. Takadoum, Corrosion Science, 38 (1996) 643.
[10] S. Mischler and **P. Ponthiaux**, Wear 248 (2001) 211.
[11] S.W. Watson, F.J. Friedersdorf, B.W. Madsen and **S.D. Cramer**, Wear, 181-183 (1995) 476.
[12] F. Assi and H. Böhni, Tribotest Journal 6 (1999) 17.
[13] P. Ponthiaux, F. Wenger, J. Galland, G. Lederer and **N. Celati**, Matériaux & Techniques, Numéro hors série, Juillet 1997, p 43.
[14] P. Jemmely, S. Mischler and **D. Landolt**, Wear 237 (2000) 63.
[15] I. Garcia, D. Drees and **J.P. Celis**, Wear 249 (2001) 452.
[16] S. Mischler, S. Debaud and **D. Landolt**, J. Electrochem. Soc. 145 (3) (1998) 750.
[17] L. Benea, P. Ponthiaux, F. Wenger, J. Galland, D. Hertz, J. Y. Malo; Wear, Wear Modelling, 256, 9-10, (2004) 948-953.
[18] A. Berradja, F. Bratu, L. Benea, G. Willems and **J.-P. Celis**; Wear, Volume 261, Issue 9, 20 November 2006, Pages 987-993.
[19] R. Oltra, in "Wear-Corrosion Interactions in Liquid Media" edited by A. A. Sagües and E. I. Meletis, Minerals, Metals and Materials Soc. (1991) 3.
[20] Lidia Benea, François Wenger, Pierre Ponthiaux; CD ROM Proceeding of EMCR 2006 - Electrochemical Methods in Corrosion Research 18 Jun 2006 - 23 Jun 2006 Dourdan, France.
[21] Benea L., Iordache V. E., Wenger F., Ponthiaux P., Peybernes J., Vallory J.; The Annals University of Galati, Fascicle VIII Tribology, pp. 5-10; 2005, ISSN 1221-4590.
[22] M. Keddam, O. R. Mattos, H. Takenouti, J. Electrochem. Soc. 128 n 2 (1981) 257.
[23] I**. Epelboin, C. Gabrielli, M. Keddam, H. Takenouti**, in "Electrochemical Corrosion Testing", ASTM Special Technical Publications n 727 (1981) 150.
[24] F. Wenger and J. Galland, Electrochimica Acta 35 n 10 (1990) 1573.